Stem Cell Research 60 (2022) 102665

Contents lists available at ScienceDirect

Stem Cell Research

journal homepage: www.elsevier.com/locate/scr

# A kainic acid-induced seizure model in human pluripotent stem cell-derived cortical neurons for studying the role of IL-6 in the functional activity

Ropafadzo Mzezewa [a], Johanna Lotila [a], Heikki Kiiski [b], Andrey Vinogradov [a], Fikret Emre Kapucu [a], Jukka Peltola [c], Sanna Hagman [a], Susanna Narkilahti [a,*]

[a] Neuro Group, Faculty of Medicine and Health Technology, Tampere University, 33520 Tampere, Finland
[b] Tampere University Hospital, Department of Intensive Care, Tampere, Finland
[c] Department of Neurology, Tampere University Hospital and Faculty of Medicine and Health Technology, Tampere University, Tampere, Finland

ARTICLE INFO

*Keywords:*
Cortical neurons
Disease modeling
Interleukin 6
Human pluripotent stem cells
Microelectrode arrays
Seizures

ABSTRACT

Human pluripotent stem cell (hPSC)-derived neural cultures have attracted interest for modeling epilepsy and seizure-like activity in vitro. Clinical and experimental evidence have shown that the multifunctional inflammatory cytokine interleukin (IL)-6 plays a significant role in epilepsy. However, the role of IL-6 in neuronal networks remains unclear. In this study, we modelled seizure-like activity in hPSC-derived cortical neurons using kainic acid (KA) and explored the effects of IL-6 and its counterpart, hyper-IL-6 (H-IL-6), a fusion protein consisting of IL-6 and its soluble receptor, IL-6R. In the seizure-like model, functionally mature neuronal networks responded to KA induction with an increased bursting phenotype at the single electrode level, while network level bursts decreased. The IL-6 receptors, IL6R and gp130, were expressed in hPSC-derived cortical neurons, and the gene expression of IL6R increased during maturation. Furthermore, the expression of IL-6R increased not only after IL-6 and H-IL-6 treatment but also after KA treatment. Stimulation with IL-6 or H-IL-6 was not toxic to the neurons and cytokine pretreatment did not independently modulate neuronal network activity or KA-induced seizures. Furthermore, the increased expression of IL-6R in response to IL-6, H-IL-6 and KA implies that neurons can respond through both classical and trans-signaling pathways. Acute treatment with IL-6 and H-IL-6 did not alter functional activity, suggesting that IL-6 does not affect the induction or modulation of newly induced seizures in healthy cultures. Overall, we propose this model as a useful tool to study seizure-like activity in neuronal networks in vitro.

## 1. Introduction

Epilepsy is a complex neurological disorder that affects over 65 million people in all age groups worldwide (Devinsky et al., 2018). It is characterized by unpredictable, reoccurring seizures caused by hyperexcitable or hypersynchronous neuronal activity (Devinsky et al., 2018; Sirven, 2015). Current antiepileptic drugs are refractory in one-third of patients (Perucca et al., 2007). Therefore, new epileptic drugs are urgently required. Today, many preclinical studies are conducted in rodent models, and concerns about relevance and cost are often debated (Easter et al., 2009; Grainger et al., 2018). Better tools for the preclinical stage are therefore needed for drug development or disease modeling which would reveal the mechanism of actions of drug candidates. These human cell-based models would improve the selection of the most potential drugs for the preclinical animal trials. Human pluripotent stem cells (hPSCs) have been shown to be a promising avenue for disease modeling, drug screening and development, and toxicity analysis (Avior et al., 2016). Disease specific human induced pluripotent stem cell (hiPSC) models exist for genetic epilepsies as well as genetic disorders where epilepsy is a comorbid feature (Hirose et al., 2020). Furthermore, hPSC-derived neural cells have been suggested as a competent model next to traditional in vitro and ex vivo models (Magalhães et al., 2018; Valente et al., 2021)as well as in vivo animal models for preclinical seizure liability studies, as they mimic human cell-specific properties (Grainger et al., 2018; Ishibashi et al., 2021).

In vitro, seizure-like activity has been typified with

*Abbreviations:* hPSC, human pluripotent stem cells; hiPSC, human induced pluripotent stem cells; hESC, human embryonic stem cells; MEA, microelectrode array; KA, Kainic acid; IL-6, interleukin-6; H-IL-6, hyper-IL-6; DIV, days in vitro; PSD 95, post synaptic density-95; CNS, central nervous system.

* Corresponding author.
*E-mail address:* susanna.narkilahti@tuni.fi (S. Narkilahti).

https://doi.org/10.1016/j.scr.2022.102665
Received 18 June 2021; Received in revised form 9 January 2022; Accepted 11 January 2022
Available online 17 January 2022

hypersynchronous or hyperexcitability of neuronal firing (Jiruska et al., 2013; Liu et al., 2019). On the contrary, some studies have reported distinctive firing patterns showing disruption in network synchrony (Bradley et al., 2018). Though modeling seizures in vitro may be complicated, measuring changes in specific parameters of neuronal network activity may reflect in vivo seizures (Tukker and Westerink, 2021). Microelectrode arrays (MEAs) are a useful tool to measure and characterize extracellular neuronal network activity in vitro (Paavilainen et al., 2018; Kumar et al., 2017; Odawara et al., 2016; Mäkinen et al., 2018; Saavedra et al., 2021) and thus can be used to detect seizure-like activity (Odawara et al., 2016; Pelkonen et al., 2020). Unlike conventional electrophysiological techniques such as patch clamp or calcium imaging, which are typically invasive, MEAs allow for noninvasive and repeated measurements of neuronal networks over extended periods (Grainger et al., 2018; Saavedra et al., 2021; Niu and Parent, 2020). Seizures can be induced with pharmacological agents such as kainic acid (KA), an analog of the excitotoxic neurotransmitter glutamate (Barker-Haliski and White, 2015). KA has been used to promote bursting activity in both mouse and human neuronal cultures (Ishibashi et al., 2021; Odawara et al., 2016; Chai et al., 1991). Typically, the utilized hPSC-derived neuronal models, however, require prolonged culturing times and rodent-derived astrocytes as supporting cell types for functional maturation (Odawara et al., 2016).

The pathogenesis of epilepsy is associated with neuronal damage, gliosis and severe inflammatory responses in the central nervous system (CNS) (Vezzani et al., 2019). Inflammatory cascades are typically activated after glial cells, neurons and endothelial cells respond to various insults or seizures that lead to the secretion of inflammatory mediators such as cytokines and chemokines (Vezzani et al., 2019; Patel et al., 2019; Rana and Musto, 2018). Aberrant expression of cytokines and chemokines have been detected in epileptic patients and in animal models of epilepsy (Li et al., 2010; Lehtimäki et al., 2011). Among these cytokines, the most studied are interleukin (IL)-1β, tumor necrosis factor (TNF)-α and IL-6 (Li et al., 2010). IL-6 levels have been shown to be increased after seizures in animal models and organotypic slice cultures (Magalhães et al., 2018; Li et al., 2010) and in both cerebrospinal fluid (CSF) and plasma from epileptic patients experiencing recurrent seizures (Lehtimäki et al., 2011; Alapirtti et al., 2009; Alapirtti et al., 2018; Liimatainen et al., 2009). Moreover, patients with temporal lobe epilepsy (TLE), a type of epilepsy that is refractory to drug treatments, had elevated serum levels of IL-6 compared to those of patients with extra-TLE (Alapirtti et al., 2009; Liimatainen et al., 2009; Curia et al., 2014), suggesting the important role of IL-6 in this particular type of epilepsy.

IL-6, a pleiotropic inflammatory cytokine, is known to have multiple functions in inflammation, immune defense and tissue regeneration (Rothaug et al., 2016), and in the CNS, it is known to modulate neuronal and synaptic functions (Gruol, 2015). IL-6 influences biological processes through two receptors, a ligand-binding membrane-bound glycoprotein, IL-6R (CD126), and a transmembrane protein, gp130 (Kaur et al., 2020). Gp130 is ubiquitously expressed in almost all cell types, while IL-6R expression is more limited, for example, to leukocytes, hepatocytes, epithelial cells, and microglia (Rothaug et al., 2016; Kaur et al., 2020; Rose-John, 2017). Through these receptors, IL-6 activates either the classical or trans-signaling pathway (Rothaug et al., 2016; Kaur et al., 2020; Rose-John, 2017). In the classical signaling pathway, IL-6 binds to membrane-bound IL-6R, initiating dimerization of gp130 and consequently activating downstream signals (Rothaug et al., 2016). Alternatively, IL-6 can form a complex with soluble IL-6R (sIL-6R) in the absence of membrane-bound IL-6R and thus activate gp130, leading to the trans-signaling pathway (Rothaug et al., 2016). To model the trans-signaling pathway in vivo and in vitro, a designer fusion protein named hyper-IL-6 (H-IL-6) has been developed (Rose-John, 2017; Fischer et al., 1997). In this fusion protein; IL-6 and sIL-6R are covalently linked by a peptide chain (Fischer et al., 1997); and this compound has been successfully used to activate the gp130-mediated trans-signaling pathway (Rose-John, 2017).

Here, we model seizure-like activity in vitro in functional hPSC-derived cortical neurons using KA as the seizure-inducing agent. We characterized the expression of IL-6R and gp130 in developing neuronal networks to confirm that the neurons were responsive to IL-6 or its fusion protein, H-IL-6. We showed that the expression of IL-6R was significantly increased in cortical neurons in response to treatment with IL-6, H-IL-6 and KA. We investigated the potentiating or alleviating effects of IL-6 or H-IL-6 administered alone or in combination with KA treatment on hPSC-cortical neurons. In the utilized paradigm, IL-6 or H-IL-6 did not cause seizure-like activity alone or worsen the KA-induced seizure phenotype.

## 2. Methods

### 2.1. Human pluripotent stem cells and differentiation of cortical cultures

The main study was conducted with neuronal cells derived from the human induced pluripotent stem cell (hiPSC) line 10212.EURCCs (Kiamehr et al., 2019). Some of the results were further verified with neuronal cells derived from a human embryonic stem cell line (hESC; Regea 08/023) (Skottman, 2010). The Faculty of Medicine and Health Technology has received a supportive statement from the regional ethics committee of Pirkanmaa Hospital District for the derivation; culture, and differentiation of hESCs and hiPSCs (R05116, R08070, R12123). Informed consent was obtained from the subjects who donated the cell samples. hiPSCs were expanded and differentiated into cortical neurons in a feeder-free culture, as previously described (Hongisto et al., 2017; Hyvärinen et al., 2019). Briefly; during induction days in vitro (DIV) 0–12, the neuronal maintenance medium was supplemented with the small molecules LDN193189 (100 nM) and SB431542 (10 μM, Sigma). In the neural proliferation stage (days 13–25), neural maintenance medium was supplemented with fibroblast growth factor-2 (FGF2, 20 ng/ml, Thermo Fisher Scientific). In the final maturation stage (days 26–69), neural maintenance medium was supplemented with essential growth factors comprising brain-derived growth factor (BDNF, 20 ng/ml, R&D Systems), glial-derived neurotrophic factor (GDNF, 10 ng/ml, R&D Systems), dibutyryl cyclic adenosine monophosphate (db-cAMP, 500 mM, Sigma-Aldrich) and L-ascorbic acid (AA, 200 mM, Sigma-Aldrich) and was thus termed neural maturation medium. DIV 32 was considered the start of experiments when cells were plated for culture and MEA plates (Fig. 1A). Neurons were plated at a density of 50 000 cells/cm$^2$ in poly-L-ornithine (PLO)- and human recombinant laminin LN521 (Biolamina, Sweden)-treated cell culture plates (Thermo Fisher Scientific). MEA plates 48 array format, Axion BioSystems, Atlanta, GA, USA) were pretreated first with a 10 ml droplet of 0.1% polyethylenimine (PEI, Sigma-Aldrich) in 0.1 M borate buffer and then with a 10 ml droplet of 50 mg/ml LN521 (Biolamina). Then, 80 000 cells in a 10 μl droplet (cell density 635 000 cells/cm$^2$) were plated on the MEAs. The cultures were kept in neural maturation medium and cultured at + 37 °C in a 5% $CO_2$ humidified incubator. Media for neurons were refreshed four times a week.

### 2.2. Epilepsy modeling using KA following cytokine pretreatment

KA (5 μM, K0250, Sigma-Aldrich) was used as the seizure-inducing compound in the cultures at DIV 68. The KA-induced changes in neuronal network functionality were followed for 24 h. In the second setup, the cells were pretreated with either IL-6 (100 ng/ml, PeproTech) or H-IL-6 (100 ng/ml, a kind gift from Prof. Dr. Stephan Rose-John, Kiel University, Germany) at DIV 67 for 24 h prior to KA treatment and followed for another 24 h, thus a total treatment time of 48 h. The experimental groups were as follows: KA, IL-6, H-IL-6, IL-6 plus KA, H-IL-6 plus KA, and control groups.

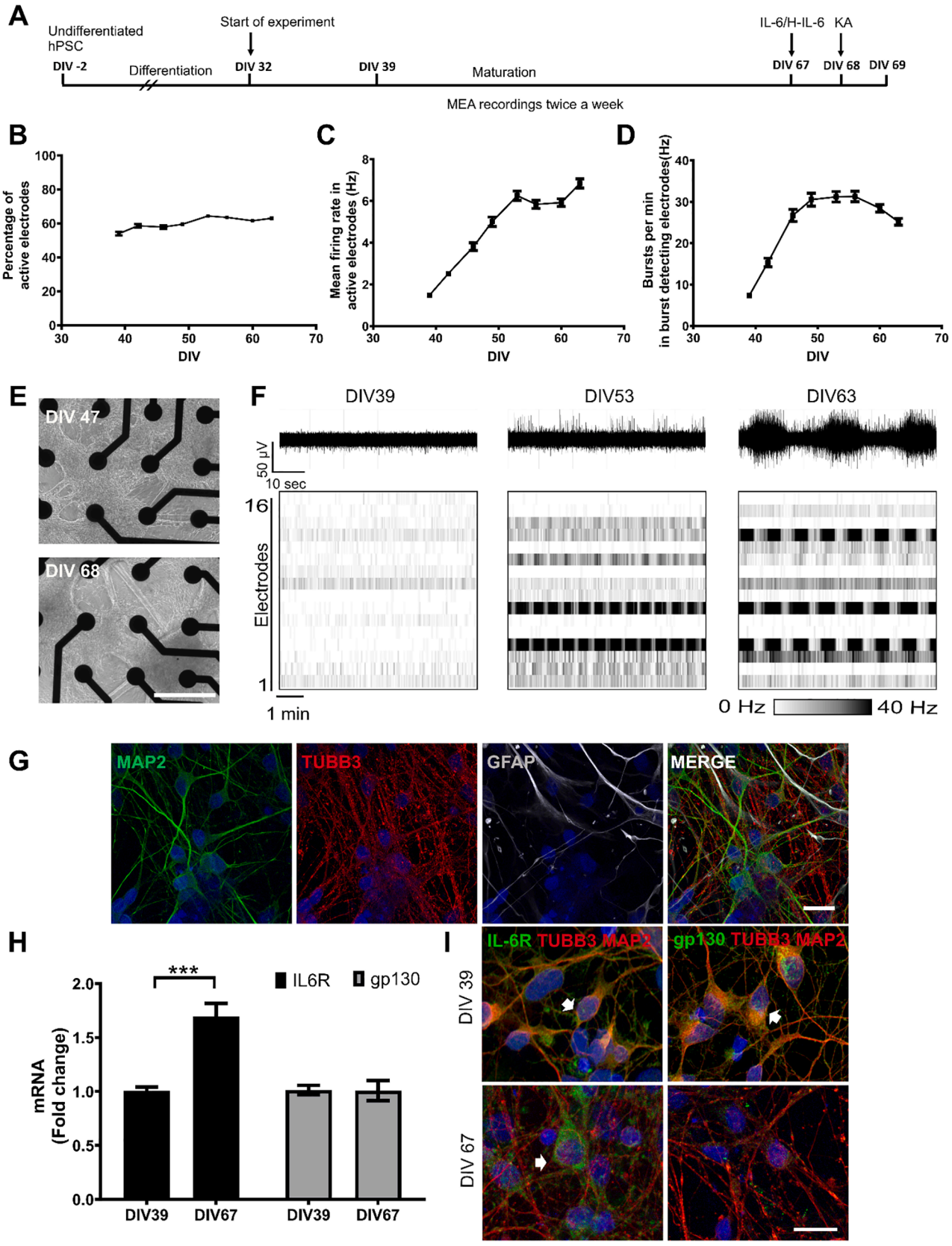


*(caption on next page)*

**Fig. 1.** Experimental outline and functional development of hiPSC-derived cortical neurons. **(A)** Experimental outline of the study. **(B)** Percentage of active electrodes (electrodes detecting spikes) over time. Electrodes considered active detected > 10 spikes/min. **(C)** Mean firing rate (spike rate) of the active electrodes (Hz) showing development in cortical networks over time and **(D)** Burst per min (burst rate) (Hz) development in the burst detecting electrodes. Data expressed as the mean ± SD (n = 192 wells). **(E)** Phase contrast images showing the morphology of cortical networks growing on top of electrodes in the MEA. **(F)** Representative images of raw data from single electrodes detecting spikes over time. Below, representative raster plots of a single MEA containing 16 electrodes show the intensity of spiking activity development over time. Raster plots are shown in 10 min segments. **(G)** Characterization of cortical neuronal cultures at 5 weeks (DIV67) showing the presence of both neurons and astrocytes in the cultures. **(H)** Gene expression of the IL-6 receptors IL-6R and gp130 at DIV 39 and DIV 67. Data are presented as the mean with +/- SEM (two experimental repeats with n = 2–3 technical replicates in each group). The Mann-Whitney *U* test with Bonferroni correction was used to determine statistical significance between the two timepoints of each receptor group (***p < 0.001, **(I)** Expression of the IL-6 receptors IL-6R and gp130 in cortical neurons at DIV 39 and DIV 67. The scale bar is 200 μm.

### 2.3. RNA isolation and quantitative PCR

RNA was isolated with a NucleoSpin RNA kit (Macherey-Nagel, Düren, Germany). The concentration and purity of RNA were quantified with a NanoDrop 1000 (Thermo Fisher Scientific). 200 ng reaction of RNA was converted to cDNA using a High Capacity cDNA Reverse Transcription Kit (Thermo Fisher Scientific). The expression levels of IL-6R (Hs01075664_m1) and gp130 (Hs00174360_m1), GRIK and GRIA subunits, see Supplementary Table S1, were analyzed with TaqMan assays using an ABI Prism 7300 real-time PCR system (Thermo Fisher Scientific). Each 15 μl reaction contained 15 ng cDNA, 0,75 μl 20 × TaqMan Gene Expression Assay and 7 μl 2 × TaqMan Gene Expression Master Mix. The data were analyzed using the delta-delta Ct method using beta-glucuronidase (GUSB) as an endogenous control (Hyysalo et al., 2017). RNA samples were prepared in two separate experiments; and in each experiment, RNA was collected from 4 to 6 wells at DIV39 and DIV 67 prior to any treatment and at the experimental endpoint, with 2–3 wells pooled together. All the samples were run in triplicate, and data are presented with technical replicates.

### 2.4. Cell viability assay

The LIVE/DEAD viability/cytotoxicity kit for mammalian cells (Thermo Fisher Scientific) was used to assess the cytotoxic effects of KA, IL-6, or H-IL-6 treatment on neurons, as previously described (Hyysalo et al., 2017). The viability was performed on mature neuronal cultures (Supplementary S3C). After treatment, the cultures were incubated for 30 min at room temperature (RT) with calcein-AM (0.1 mM) to visualize live cells and ethidium homodimer-1 (EthD-1, 0.5 mM) (all from Thermo Fisher Scientific) to visualize dead cells. Samples were imaged immediately with an Olympus IX51 equipped with an Olympus DP30BW Microscope Digital Camera (Olympus Corporation, Shinjuku, Tokyo, Japan). Images were quantified with CellProfiler software 3.1.8 (Carpenter et al., 2006); and the areas of live and dead cells were quantified as previously described (Hyysalo et al., 2017). For analysis, 4 images were taken from each well, and 3–4 wells/group were used.

### 2.5. Immunocytochemistry

Immunocytochemistry was performed as previously described (Lappalainen et al., 2010). Briefly; cells were blocked with 10% normal donkey serum, 0.1% Triton X-100 and 1% bovine serum albumin in PBS, at room temperature for 45 min. The samples were then incubated overnight at + 4 °C with primary antibodies: anti-Tubulin beta-3 chain (TUBB3, chicken, 1:200, Abcam: ab41489), anti-microtubule-associated protein 2 (MAP2, rabbit, 1:400, Millipore: AB5622), anti-MAP2 (chicken, 1:400, Novus Biologicals: NB300-213), anti-glial fibrillary acidic protein (GFAP, chicken, 1:4000, Abcam: ab4674), anti-synaptophysin (Syn, rabbit, 1:500, Abcam: ab32127), anti-postsynaptic density protein 95 (PSD95, mouse, 1:50, Abcam: ab2723), anti-IL-6Ra (mouse, 1:200, R&D Systems: MAB2271), and anti-gp130 (mouse, 1:50, Santa Cruz: sc-376280). Thereafter, the samples were incubated at RT for an hour with Alexa Fluor-labeled secondary antibodies: donkey anti-rabbit 488 (A21206), donkey anti-mouse 488 (A21202), donkey anti-rabbit 568 (A10042), donkey anti-mouse 568 (A10037), goat anti-chicken 568 (A11041), donkey anti-rabbit 647 (A31573) and goat anti-chicken 647 (A21449) (diluted 1:200 or 1:400, all from Thermo Fisher Scientific). Prior to immunolabeling for anti-IL-6Ra and anti-gp130, the quality of the antibodies was evaluated by testing at least three different concentrations and with antibody blocking test which showed decrease of staining with increasing blocking peptide concentration (data not shown). For fluorescence imaging, an Olympus IX51 inverted fluorescence microscope was used. Confocal imaging was performed using an LSM 780 laser scanning confocal microscope (Zeiss).

### 2.6. Microelectrode array (MEA) measurements

Neuronal network activity was recorded with an Axion Maestro system controlled by AxIS Software (Axion Biosystems) with a 12.5 kHz sampling rate. Recordings were obtained under a controlled temperature of 37 °C. The development of spontaneous activity was recorded twice a week with 10 min recordings until the synchronous network activity phase was reached at DIV 67. Prior to all recordings, MEA plates were allowed to equilibrate for 5 min. Refreshment of the medium was always performed a day before the MEA measurements.

For pharmacological experiments, baseline recording was performed for 15 min prior to exposure to KA, IL-6, or H-IL-6, followed by repeated MEA measurements at 3 h, 6 h and 24 h. A total of four 48-well Axion MEA plates were used, with each plate containing samples from all the six experimental groups. Thus, each experimental group had a total of 32 MEA wells for pharmacology experiments.

### 2.7. MEA data analysis

Spike detection was performed with a previously described method (Lieb et al., 2017; Mayer et al., 2018) embedded in an in-house-made MATLAB (MathWorks) script (Hyvärinen et al., 2019). Bursts were identified locally at single electrode level from the spike timestamps with the logISI algorithm (Pasquale et al., 2010); thus, showing local population activity. The minimum number of spikes per burst was set to five, and the cut off for the interspike interval (ISI) and the default maximum ISI (maxISI) were set to 100 ms. A single modification was introduced into the algorithm: when the computed ISI threshold was smaller than the default maxISI, the bursts with an interburst interval smaller than 100 ms were merged. Spike and burst features as well as other MEA parameters, such as the number of active electrodes (electrodes with > 10 spikes/min), were computed with meaRtools per well, (Gelfman et al., 2018). Burst features were presented only for burst-detecting electrodes.

Network burst detection was based on the algorithm previously introduced by (Bakkum et al., 2013) to analyze network level synchronous activity. Briefly, the algorithm focuses on separating network firing regimes from the irregular firing. Initially, time points of all the detected spikes from every electrode in each well was combined into a single train to calculate network ISIs. Then, logarithmic ISI histogram of N consecutive spikes was calculated for each well. Only the histograms exhibiting two separated peaks represented two different firing regimes, i.e., spikes belonging to network bursting and spikes outside of network firing respectively. Thus, threshold for detecting network burst was selected in

the minimum point between these peaks. N was selected as 70 for the histogram and the minimum number of channels in a network burst was set to two. Finally, the spike trains having ISIs less than the calculated threshold were considered as network bursts.

### 2.8. Statistical analysis

Statistical analyses were performed using SPSS Statistics, Version 25.0 (IBM, Armonk, New York, USA) (IBM). Graphs were plotted with GraphPad Prism 5 (GraphPad Software, San Diego, USA). The Shapiro-Wilk test was used to evaluate the distribution, which showed that the data were not normally distributed. Therefore, Kruskal-Wallis test followed with the Mann-Whitney *U* test with Bonferroni correction was used to study the statistical significance of differences in gene expression, cell viability and MEA data. Data for MEA graphs are calculated as a percent from baseline. Raw MEA data is found in Supplementary material, excel sheet. A p-value<0.05 was statistically significant. Statistical significance is denoted as *$p < 0.05$, **$p < 0.01$, *** $p < 0.001$ and ****$p < 0.0001$.

## 3. Results

### 3.1. HiPSC-derived cortical neurons develop into mature and functional networks over time

HiPSC-derived cortical cultures were recorded with MEAs twice a week from DIV39 until DIV67 (Fig. 1A) to assess the development of spontaneous functional network activity. The recordings revealed that the percentage of active electrodes (electrodes detecting > 10 spikes/min) was relatively stable, ranging from 54 to 63%, during activity development (Fig. 1B). The mean firing rate (spiking activity) of the active electrodes steadily increased over time and reached a peak rate of 6 Hz by DIV 52 (Fig. 1C) and plateaued until DIV 63. Similarly, the bursts per minute (burst rate) of the burst detecting electrodes increased substantially, starting from the first recordings, and peaking at DIV 52 with a rate of 31 Hz. Thereafter, the burst rate remained constant and slightly declined to 25 Hz by DIV 63 (Fig. 1D). The representative phase contrast images showed that the hiPSC-derived cortical neurons formed dense cultures in the MEAs (Fig. 1E). The development of activity was also visible in the organization of spikes. In their immature state (DIV 39), few spikes were detected and fired randomly, as seen both at the single-electrode level and in raster plots (Fig. 1F). This spiking phenotype changed with increased culture time and portrayed a more mature phenotype as spike trains assembled into bursts with synchronous firing by DIV 63 (Fig. 1F). Furthermore, immunocytochemical characterization of cortical cultures at DIV 67 showed that the cultures expressed microtubule-associated protein 2 (MAP2, a marker for mature neurons), Tubulin beta-3 chain (TUBB3, a pan-neuronal marker) and glial fibrillary acidic protein (GFAP, an astrocytic marker) (Fig. 1G). These results indicate that the cultures consisted of mature neuronal networks.

In addition, the gene and protein expression of the IL-6 receptors IL-6R and gp130 was evaluated at DIV 39 (immature stage) and DIV67 (mature stage, Fig. 1A) using RT-qPCR and immunocytochemistry. Gene expression analysis indicated that cortical neurons expressed both receptors early in culture, and the expression of IL-6R significantly increased ($p < 0.001$) at maturation, while gp130 expression remained relatively stable (Fig. 1H). However, at the immature stage, DIV 39, the Ct value revealed that gp130 expression was higher than IL-6R expression (Supplementary Fig. S1A). At the protein level, both receptors were expressed in cortical neurons during the immature stage (DIV 39), and expression was mostly detected in the perinuclear area (Fig. 1I). As the networks matured, the expression of IL-6R remained in the perinuclear area, while the expression of gp130 was reduced and localized to neurites (Fig. 1I). Taken together, these data indicate that neuronal networks can be cultured over the course of time and that they develop functional maturity across MEAs and express both IL-6 receptors.

### 3.2. Kainic acid induces seizure-like activity in cortical human neurons

To model epileptic seizures, functionally mature networks that displayed bursting behavior were treated with KA at DIV 68 for 24 h. Prior to treatment with KA, gene expression of kainate and AMPA receptors in cortical neurons were analyzed to ensure that the cultures could respond to the treatment (Supplementary Fig. S1B). The effect of KA on neuronal network activity was monitored with MEA measurements directly after its addition (acute) and 3 h, 6 h, and 24 h thereafter. At the single electrode level, KA treatment increased the bursting activity in the cultures from the acute time point timepoint ($p < 0.0001$) until 6 h after KA treatment ($p < 0.05$), while no change was detected at the 24 h timepoint (Fig. 2A). The burst durations were significantly shorter (bursting frequencies, ($p < 0.05$), in KA-treated cultures in all time points (Fig. 2B). Furthermore, the mean inter-burst-intervals (IBI) was reduced following acute treatment ($p < 0.0001$) but increased after 24 h ($p < 0.01$, Fig. 2C), illustrating that the acute treatment of KA exhibited more frequent, shorter bursts while prolonging the burst frequency toward the endpoint. The KA treated cultures also demonstrated a reduction in the mean firing rate (spike rate) at all timepoints following KA treatment ($p < 0.0001$ in all time points, Fig. 2D as with the number of spikes in bursts ($p < 0.001$, Supplementary Fig. S2). At the network burst level, the analysis revealed that KA significantly diminished network wide synchronous activity directly after addition (acute) until 24 h, compared to control cultures (Fig. 2E, F). The network burst raster plots (Fig. 2E), however, showed that the original bursts were disrupted into rapid firing, rendering them undetectable as synchronous network bursts. Overall, the cultures responded to KA treatment in a manner that typified seizure-like behavior and consequently modeled epileptic activity in vitro.

### 3.3. Cytokine and KA treatments induce increased expression of IL-6 receptors in cortical human neurons, and the cells remain viable

As IL-6 has been associated with pathological alterations in patients with recurrent seizures (Lehtimäki et al., 2011; Alapirtti et al., 2009), we investigated the functional implications of IL-6 for our cortical neurons. Prior to this, the potential toxicity of the cytokine was investigated. A LIVE/DEAD assay was used to investigate the effect of IL-6 or H-IL-6 treatment, together with KA treatment, on the viability of cortical neurons. A substantial number of viable cells (green) and only a few dead cells (red) were detected in each experimental group (Fig. 3A). The number of live and dead cells was quantified based on the percentage of area coverage. There were no significant differences in viability when the treatment groups were compared to the control group (Fig. 3B), indicating that none of the treatments were cytotoxic. This was also confirmed in the hESC-derived cortical neuronal cell line (Supplementary Fig. 3A).

To understand whether cytokine treatments modulate the expression of IL-6R and gp130, the gene expression of these receptors was evaluated (Fig. 3C). There was an increase in the gene expression levels of IL-6R in all treatment groups compared to the control group ($p < 0.001$, Fig. 3C), while no significant alterations in gp130 gene expression were observed. The hESC-derived cortical neurons showed a similar trend for IL-6R; H-IL-6- and H-IL-6 + KA-treated cultures exhibited an upregulation of IL-6R receptor levels ($p < 0.0001$), while gp130 expression was upregulated in IL-6-, H-IL-6- and H-IL-6 + KA-treated cultures ($p < 0.05$, $p < 0.0001$ and $p < 0.0001$, Supplementary Fig. 3B). Taken together, these results show that the neurons responded to cytokine and KA treatments by notably expressing the IL-6R gene at concentrations that were not cytotoxic to cells.

### 3.4. Cytokine treatment does not modulate the functionality of human cortical networks

Since IL-6 treatment was not cytotoxic to neural cells, we then

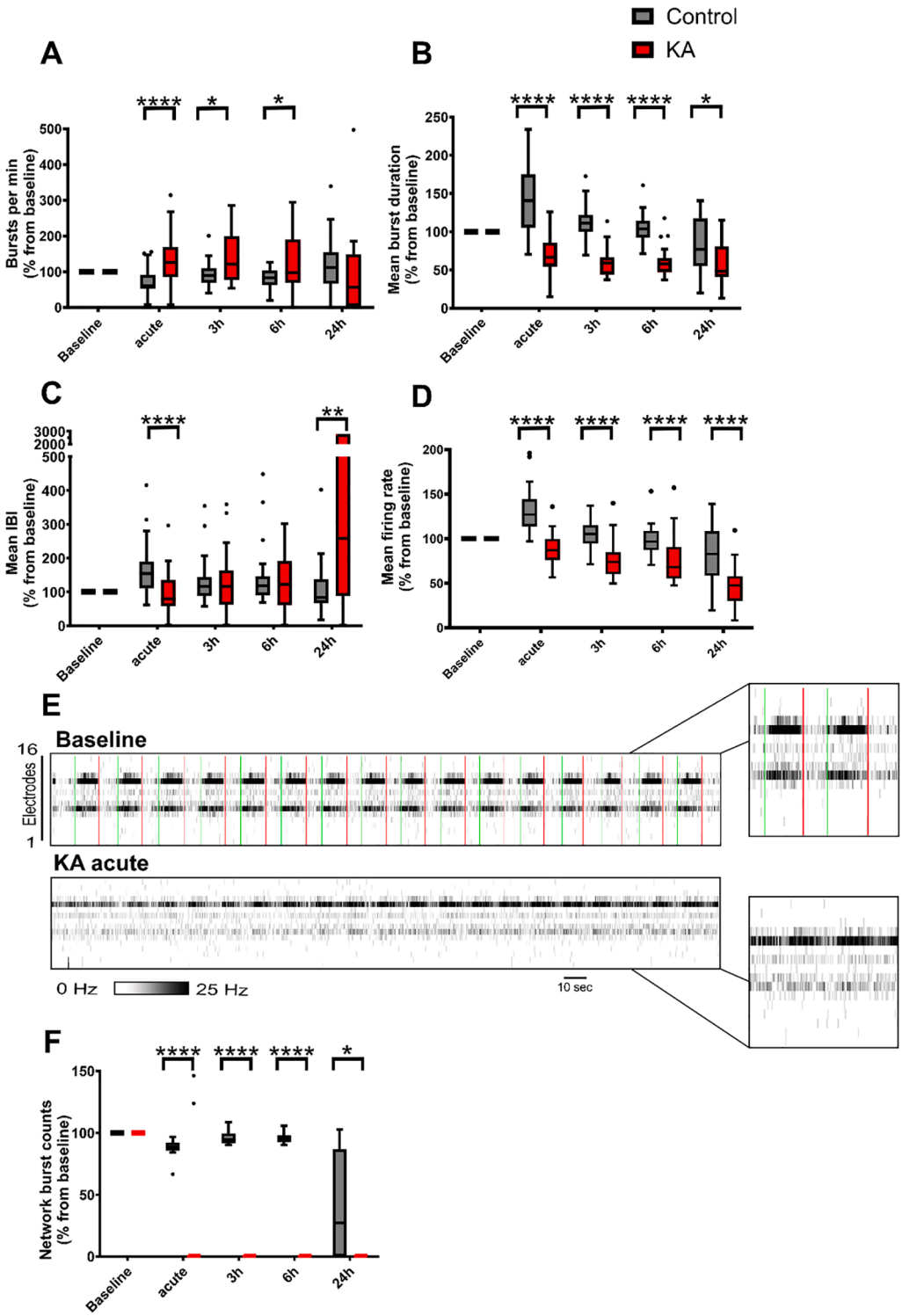


**Fig. 2.** Seizure-like activity modelling in cortical neurons using kainic acid (KA). **(A)** A significant increase in bursts per minute (bursts per min) from the time of induction until 6 h timepoint. **(B)** A shorter mean burst durations in KA-treated cultures compared to the control cultures at all timepoints and **(C)** a significant decrease in the inter-burst intervals (IBI) at acute timepoint and 24 h. **(D)** A reduction in the mean firing rate in KA-treated cultures at all time points. **(E)** Exemplary raster plots exhibiting changes in synchronous network burst activity from baseline to acute treatment of KA. The green and red vertical lines are drawn automatically by the algorithm to show beginnings and endings of detected network bursts respectively. The raster plots, with zoomed segments, presents the perturbed synchronous network bursting activity following KA application (i.e., no detected network bursts), which was previously seen at baseline. **(F)** Quantified data showing significant loss of network bursts counts in KA treated samples compared to control at all time points. Variation of data visible at 24 h timepoint. Data for all graphs were calculated as percentages from baseline. The number of recorded MEA wells/experimental group was 32. Data are expressed as Tukey box plots, and outliers are shown with black circles. The Mann-Whitney *U* test with Bonferroni correction was used to determine statistical significance between KA-treated and controls groups (*$p < 0.05$, **$p < 0.01$, ***$p < 0.001$, ****$p \leq 0.0001$. (For interpretation of the references to colour in this figure legend, the reader is referred to the web version of this article.)

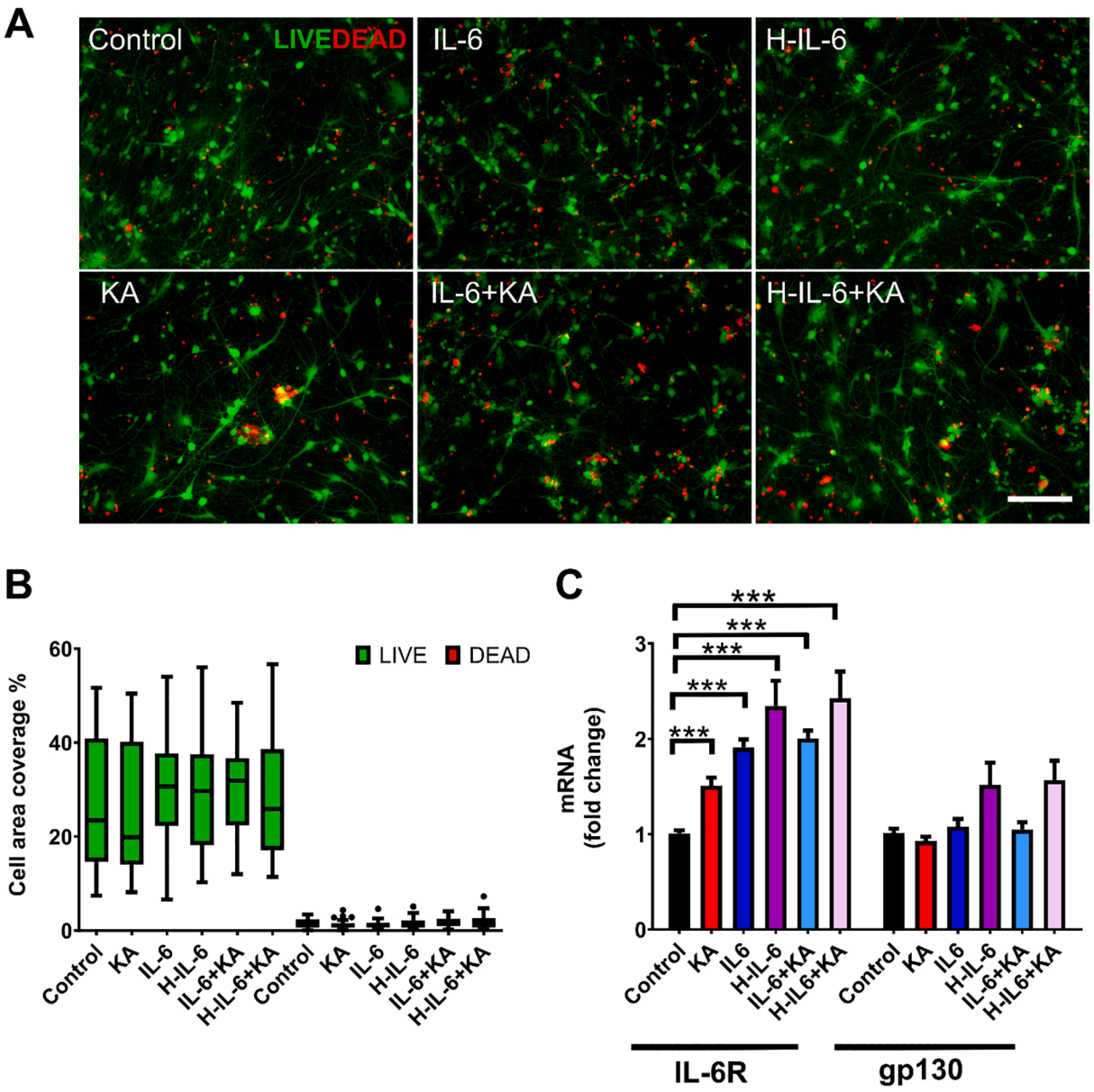


**Fig. 3.** Cell viability and IL-6 receptor gene expression after cytokine and KA treatments. **(A)** Representative images of live/dead staining after treatments. **(B)** Quantification of cell viability based on area coverage in experimental groups. Data for live/dead staining are presented as Tukey box plots of area coverage within the total culture area (n = 26–30 images per group). **(C)** Gene expression of the IL-6 receptors IL-6R and gp130 after treatment. Kruskal-Wallis test followed with Mann-Whitney *U* test with Bonferroni correction was used to determine statistical significance between experimental groups in comparison to the control group (***$p < 0.001$). The scale bar is 100 μm.

assessed whether IL-6 or H-IL-6 influenced neuronal network activity. For this purpose, functionally mature cultures at DIV67 were treated for 24 h with IL-6 or H-IL-6. After baseline recording, IL-6 and H-IL-6 were added to the cultures, and neuronal network activity was measured directly after addition (acute) and 3 h, 6 h and 24 h thereafter (Fig. 4A). IL-6 or H-IL-6 treatment did not evoke changes in the mean firing rate activity (Fig. 4B), spike rate) or burst per min (Fig. 4C, burst rate) compared to those of control cultures. In summary, the cytokine compounds did not independently modulate the functional activity of human cortical networks.

### 3.5. Cytokines do not potentiate KA-induced seizures in neuronal cultures

Next, cultures were treated with KA after pretreatment with IL-6 or H-IL-6 to determine whether cytokines modulate KA-induced seizures. Pretreatment with IL-6 and H-IL-6 induced no functional alterations compared to cultures treated with KA alone and instead showed similar trends, with a moderate decrease in the mean firing rate (Fig. 4D), shorter bursts (Fig. 4E) and slightly increased burst frequencies over time (Fig. 4F). The expression of synaptic structures enabling synaptically driven activity was confirmed in all the treatment groups. Synaptic structures were detected with the pre- and postsynaptic markers synaptophysin and PSD-95, respectively. Synaptic puncta were detected in proximity to each other during neuronal processes in all treatment groups (Fig. 5). The results demonstrated that the cytokine compounds did not induce any functional alterations or suppress seizure-like behavior in cultures treated in combination with KA exposure.

## 4. Discussion

In this study, we modeled seizure-like activity in vitro in functional hPSC-derived cortical neurons using KA as the seizure-inducing agent

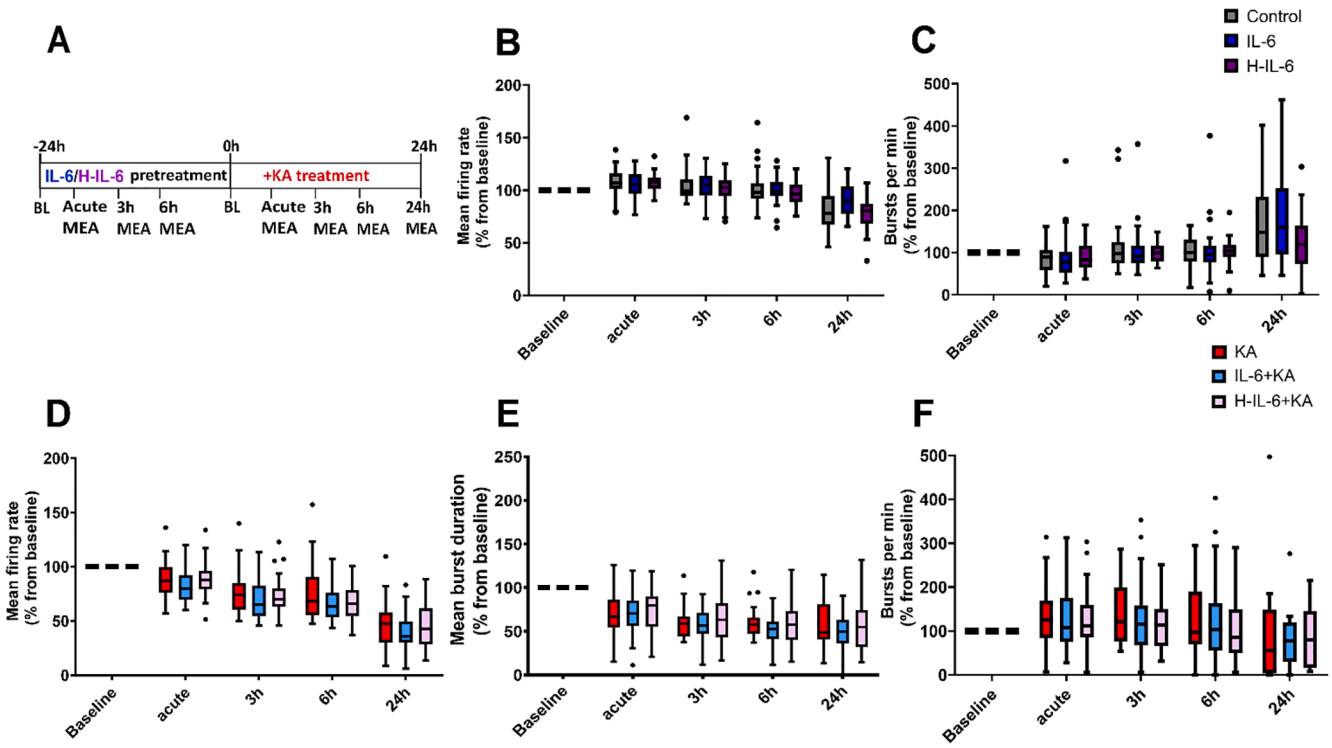


**Fig. 4.** Effect of IL-6/H-IL-6 on the functionality of the KA model. **(A)** Outline of the experimental treatments. A baseline measurement was conducted for 15 min prior to both cytokine (acute) and KA induction, followed by MEA measurements at 3 h, 6 h and 24 h. **(B)** Mean change in firing rate (spike rate) and **(C)** burst per min (burst rate) over time following cytokine treatment. A similar decrease in overall network functionality was detected in the cytokine-pretreated cultures compared to cultures treated with KA alone, as shown in **(D)** for the mean firing rate, **(E)** mean burst duration and **(F)** bursts per min. Data for all graphs were calculated as percentages from baseline. The KA data in **(D-F)** is repeated from the KA data from Fig. 2A,B andD. The number of recorded MEA wells/experimental group was 32. Data are presented as Tukey box plots, and outliers are shown with black circles.

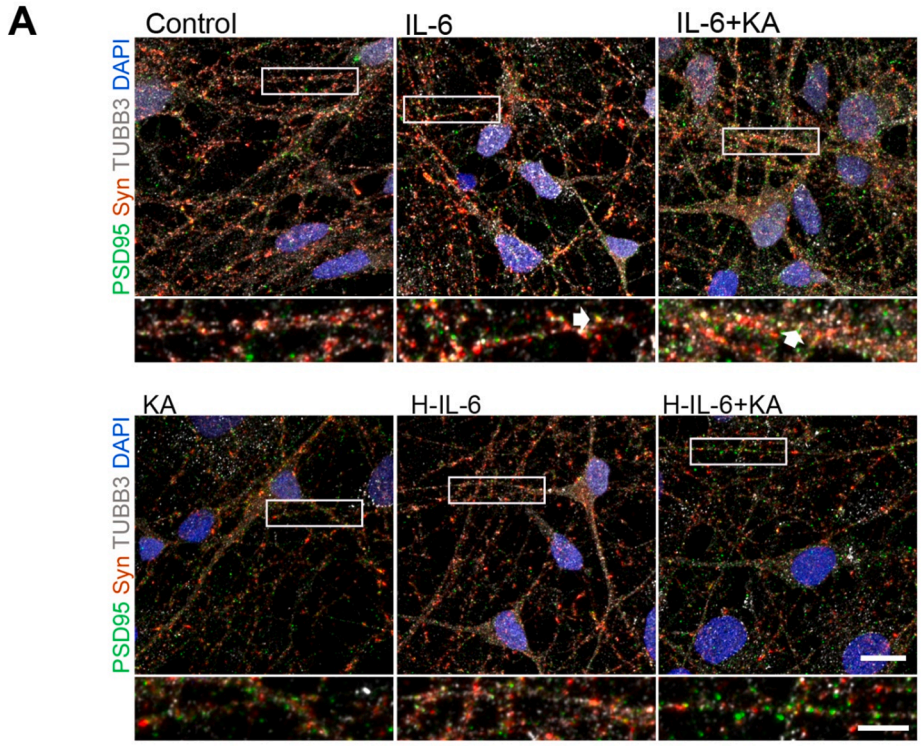


**Fig. 5.** Evaluation of synapses following cytokine and KA treatments. Immunocytochemical staining of excitatory synapses with PSD-95 (postsynaptic terminal marker) and synaptophysin (Syn, presynaptic terminal marker) in the treatment groups. The insets below show a magnified view of the neuronal processes. Arrows point to synaptic structures were pre- and postsynaptic markers are in close proximity. Scale bars are 10 μm (upper panel), and 2 μm (inset panels).

and investigated the effect of IL-6 on the network activity and viability.

Rodent brain slice assays are the gold standard for assessing the seizure liability of compounds (Authier et al., 2016). These models, however, lack high-throughput ability to simultaneously evaluate the effect of several compounds (Bradley et al., 2018). Furthermore, their relevance to humans is often debated, as the brain slice assays or cultures used are derived from rodents (Rockley et al., 2019). Therefore, hPSC-derived neurons have the potential to model seizures in a context closer to functional human neuronal networks (Grainger et al., 2018). MEA technology offers higher throughput for in vitro functional analysis; as the number of parallel samples ranges from 1 to 48 in commercially available systems (Rockley et al., 2019). Here, MEAs were utilized to monitor seizure-like activity in hPSC-derived cortical neurons. To obtain functional mature networks, hPSC-derived cortical neurons were cultured over several weeks on MEAs, as previously shown (Odawara et al., 2016; Pelkonen et al., 2020; Hyvärinen et al., 2019). During that time, spontaneous synchronous bursting activity developed, which is essential for neural circuitry formation (Zhang and Poo, 2001) and is an indicator of mature networks (Odawara et al., 2016). In the present study, maturation of the networks was observed as neurons firing several single spikes progressively organized into bursting activity that peaked at day 50 and remained relatively stable, as shown previously with similarly differentiated, non-rodent astrocytes containing neuronal cultures (Hyvärinen et al., 2019).

Excessive release of the main excitatory neurotransmitter, glutamate, is suggested to be a key factor resulting in irregular neuronal signaling and epileptic activity (Barker-Haliski and White, 2015). KA activates the AMPA/kainate receptors of glutamate and thus has been used as a seizure-inducing agent to model epilepsy both in vivo and in vitro (Chai et al., 1991; Narkilahti et al., 2003; Lehtimäki et al., 2003; Lu et al., 2019; Fezza et al., 2014). A 5 μM KA concentration was used as it was previously shown to decrease the spike rate (Hyvärinen et al., 2019) and increase burst frequency and thus hyperexcitability (Odawara et al., 2016) in hiPSCs derived neuronal networks at the single electrode level. Here, we report that modeling seizure-like events using KA in a multi-well MEA system was possible with hiPSC-derived neuronal cultures. KA exposure resulted in a remarkable increase in burst frequency with shorter burst durations and reduced inter-burst intervals, thus exhibiting more frequent and shorter bursts over time. This increased 'burstiness' pattern altered from baseline activity at the single electrode level in response to KA suggests seizure-like activity in vitro (Bradley et al., 2018; Tukker and Westerink, 2021). Moreover, the network wide synchronous bursts were diminished by KA treatment. In line, a recent study (Ishibashi et al., 2021) using hiPSC derived neurons showed alterations in several network burst parameters in relation seizurogenic compounds, including KA. Thus, the utilized KA concentration was effective in inducing a seizure-like effect in our cultures.

Furthermore, the KA concentration used did not affect cell viability, and the detection of both pre- and postsynaptic terminals confirmed synaptic-driven activity. Thus, despite that the KA model did not recapitulate the cell death feature of TLE (Costa et al., 2020) it nevertheless demonstrates the ability to model seizure-like activity in human neuronal cultures in an MEA platform.

IL-6 is an inflammatory cytokine whose expression is increased in epileptic seizures, however, its exact role is not known. The biological activity of IL-6 is mediated by its receptors, IL-6R and gp130 (Kaur et al., 2020); gp130 is ubiquitously expressed, while IL-6R expression is restricted to leukocytes, hepatocytes and microglia (Rothaug et al., 2016; Gruol, 2015; Kaur et al., 2020; Rose-John, 2017). However, a few studies have reported that both receptors are expressed at the gene and protein levels by neurons and glial cells in different brain regions in humans and rodents (Schöbitz et al., 1993; Hampel et al., 2005) and in hiPSC-derived neurons (Sulistio et al., 2018). In the present study, we confirmed the expression of both receptors in human neurons at the gene level. Notably, the expression of gp130 was higher than that of IL6R at the immature stage (see Supplementary Figure S1). During the maturation period, the gene expression of gp130 remained stable, while the expression of IL-6R increased. Previous studies have reported similar findings for IL-6-related receptors at the mRNA level in hESC-derived neural progenitors and at both the mRNA and protein levels in mouse cortical neurons (Ali et al., 2000; Hagman et al., 2019). Furthermore, the expression of gp130 and IL-6R was confirmed at the protein level, although gp130 levels were reduced and IL-6R levels increased in the late maturation stage. In relation to these differences, it is important to note that the correlation of gene and protein expression is influenced by several biological processes (Liu et al., 2016). Cellular regulation of gp130 expression has been described to include complex mechanisms that can alter its protein stability (Wolf et al., 2014).

Furthermore, when functionally mature neuronal cultures were treated with IL-6 and H-IL-6, no cytotoxic effects were detected, which is in line with our previous study with different hPSC neuronal model (Hagman et al., 2019). The data are also in line with previous reports testing IL-6 and H-IL-6 in mouse neural stem cells (Islam et al., 2009) or testing IL-6 in hiPSC-derived neural aggregates (Zuiki et al., 2017). Interestingly, treatment with IL-6, H-IL-6 and KA in mature cultures increased expression of the IL-6R gene, suggesting that the cells were able to respond to these cytokines through the classical (anti-inflammatory properties) and trans-signaling (proinflammatory properties) pathways (Rothaug et al., 2016; Wolf et al., 2014). In support of this, we previously showed that hPSC-derived neurons respond to IL-6 by secreting the anti-inflammatory factor IL-10 as well as the neurotrophic factor vascular endothelial growth factor (VEGF) (Hagman et al., 2019). We conclude that the mature cortical neurons are responsive to the cytokine IL-6 as well as KA, as they express both receptors, revealing their ability to respond to cytokine treatment.

The exact role of IL-6 in epilepsy is not known, but in vitro studies with neuronal cultures have revealed that it plays a crucial role in neuroprotection and neurogenesis (Sulistio et al., 2018; Ali et al., 2000; Ma et al., 2015). Moreover, IL-6 has been shown to support the morphological and electrophysiological maturation of hiPSC-derived neurons detected with the patch clamp technique (Sulistio et al., 2018). Here, the potential for IL-6 to induce functional alterations in neuronal network functions was investigated. Incubation with either IL-6 or H-IL-6 for 24 h did not directly modulate the activity of cortical neurons. In contrast to our study, a previous study with rodent primary sensory neurons showed an increase in spontaneous and stimulus-evoked activity responses to IL-6 treatment in a 48 h MEA follow-up (Black et al., 2018). However, when comparing outcomes between hPSCs and rodent neurons, it is worth noting that there are differences in cell responses due to species-specific behavior and the developmental states of the cultures used (Hyvärinen et al., 2019).

When evaluating the potentiating effect of IL-6 or H-IL-6 on KA-induced seizures, no difference in spiking or bursting behavior was observed compared to that of KA treatment alone. Our findings therefore suggest that IL-6 does not induce any acute functional alterations in hPSC-derived cortical neurons at the network level. Previous studies have shown both pro- and anti-convulsive effects in rodent models, e.g., IL-6 knockout mice were shown to be susceptible to KA-induced seizures (Penkowa et al., 2001). In contrast, transgenic mice with enhanced astrocyte IL-6 production were more susceptible to glutamatergic (KA and *N*-methyl-D-aspartate, NMDA)-induced seizures with increased mortality (Samland et al., 2003). In another study, IL-6 was shown to have proconvulsive properties in rats with pentylenenetrazole-induced seizures (Kalueff et al., 2004). In our previous clinical study, we hypothesized that seizures induce IL-6 production by astrocytes (Lehtimäki et al., 2009); however, whether this increased expression plays a pro- or anticonvulsive role is not known. Thus, even though a dual role involving both pro- and anticonvulsive properties has been proposed for IL-6, the precise role of IL-6 in neuronal networks is not clearly defined. Based on our findings, IL-6 and H-IL6 modulated the expression of IL-6R but did not have any potentiating effect on functional activity alone or in association with KA. This situation models a "first" seizure event in a

healthy neuronal network but does not directly model the situation in patients with an epilepsy diagnosis and a history of recurrent seizures. It, therefore, will be highly interesting to evaluate a more "chronic" and physiological seizure model with hPSC-derived cortical neurons and glial cells. In spite having a robust neuronal model, we acknowledge that the absence of the key neuroinflammatory cell types; astrocytes and microglia, are essential to observe a more predictive effect of IL-6 in epilepsy. For future studies, tri-cultures will be needed to better mimic the neuroinflammatory responses in relation to CNS diseases and deficits in vivo.

## 5. Conclusion

In this study, we demonstrated that when mature human neuronal networks are stimulated with KA they display changes in their functional phenotype that resembles seizure-like activity in vitro. We report that mature cortical neuronal networks can respond to IL-6 and H-IL-6 by modulating their expression of IL-6 receptors, thus implying an ability to respond through both classical and trans-signaling pathways. The functional effects of IL-6 alone as a potentiating agent in KA-induced seizures did not exacerbate seizure activity, which suggests that IL-6 does not affect the induction or modulation of first seizures. Overall, we can conclude that the presented neuronal model is an applicable preclinical tool for studying induced seizures and its related pathogenesis.

## 6. Ethics approval and consent to participate

The Faculty of Medicine and Health Technology has received a supportive statement from the regional ethics committee of Pirkanmaa Hospital District for the derivation, culture, and differentiation of hESCs and hiPSCs (R05116, R08070, R12123). Informed consent was obtained from the subjects who donated the cell samples.

## 7. Availability of data and materials

The datasets analyzed used/or analyzed during the study are available from the corresponding author upon reasonable request.

## Declaration of Competing Interest

The authors declare that they have no known competing financial interests or personal relationships that could have appeared to influence the work reported in this paper.

## Acknowledgements

The work was supported by the Imaging Facility, Facility of Electrophysiological Measurements and iPS Cells Facility (Faculty of Medicine and Health Technology, Tampere University). The authors also thank Biocenter Finland for the support of Imaging and iPS cells facilities. We thank Hanna Mäkelä and Eija Hannuksela for their technical assistance with cell maintenance and analyses. We kindly thank Prof, Dr, Stephan Rose-John, Kiel University, Germany, for providing us with the hyper-IL-6 fusion protein. We appreciate the technical help received from PhD Tiina Joki (Tampere University). This work was supported by the Academy of Finland (grant number 312414 to SN; 33007 to SH; 332693 (FEK), EU H2020-FETOpen (PRIME project, grant number 964712 to SN and RM), Finnish Epilepsy foundation, (RM), Instrumentarium foundation (RM), Orion foundation (RM), the Finnish Cultural Foundation (grant number 50191927 to SH), Doctoral Programme in Medicine, Biosciences and Biomedical Engineering (RM), and The Päivikki and Sakari Sohlberg Foundation (SH).

## Appendix A. Supplementary data

Supplementary data to this article can be found online at https://doi.org/10.1016/j.scr.2022.102665.

## References

Alapirtti, T., Rinta, S., Hulkkonen, J., Mäkinen, R., Keränen, T., Peltola, J., 2009. Interleukin-6, interleukin-1 receptor antagonist and interleukin-1beta production in patients with focal epilepsy: a video–EEG study. J. Neurol. Sci. 280 (1-2), 94–97.
Alapirtti, T., Lehtimäki, K., Nieminen, R., Mäkinen, R., Raitanen, J., Moilanen, E., Mäkinen, J., Peltola, J., 2018. The production of IL-6 in acute epileptic seizure: a video-EEG study. J. Neuroimmunol. 316, 50–55.
Ali, C., Nicole, O., Docagne, F., Lesne, S., MacKenzie, E.T., Nouvelot, A., Buisson, A., Vivien, D., 2000. Ischemia-induced interleukin-6 as a potential endogenous neuroprotective cytokine against NMDA receptor-mediated excitotoxicity in the brain. J. Cereb. Blood Flow Metab. 20, 956–966.
Authier, S., Arezzo, J., Delatte, M.S., Kallman, M.-J., Markgraf, C., Paquette, D., Pugsley, M.K., Ratcliffe, S., Redfern, W.S., Stevens, J., Valentin, J.-P., Vargas, H.M., Curtis, M.J., 2016. Safety pharmacology investigations on the nervous system: an industry survey. J. Pharmacol. Toxicol. Methods 81, 37–46.
Avior, Y., Sagi, I., Benvenisty, N., 2016. Pluripotent stem cells in disease modelling and drug discovery. Nat. Rev. Mol. Cell Biol. 17 (3), 170–182.
Bakkum, D.J., Radivojevic, M., Frey, U., Franke, F., Hierlemann, A., Takahashi, H., 2013. Parameters for burst detection. Front. Comput. Neurosci. 7, 193.
Barker-Haliski, M., White, H.S., 2015. Glutamatergic mechanisms associated with seizures and epilepsy. Cold Spring Harbor Perspect. Med. 5 (8), a022863.
Black, B.J., Atmaramani, R., Kumaraju, R., Plagens, S., Romero-Ortega, M., Dussor, G., Price, T.J., Campbell, Z.T., Pancrazio, J.J., 2018. Adult mouse sensory neurons on microelectrode arrays exhibit increased spontaneous and stimulus-evoked activity in the presence of interleukin-6. J. Neurophysiol. 120 (3), 1374–1385.
Bradley, J.A., Luithardt, H.H., Metea, M.R., Strock, C.J., 2018. In vitro screening for seizure liability using microelectrode array technology. Toxicol. Sci. 163, 240–253.
Carpenter, A.E., Jones, T.R., Lamprecht, M.R., Clarke, C., Kang, I.H., Friman, O., Guertin, D.A., Chang, J.H., Lindquist, R.A., Moffat, J., Golland, P., Sabatini, D.M., 2006. Cell Profiler: image analysis software for identifying and quantifying cell phenotypes. Genome Biol. 7, R100.
Chai, X., Münzner, G., Zhao, S., Tinnes, S., Kowalski, J., Häussler, U., Young, C., Haas, C. A., Frotscher, M., 2014. Epilepsy-induced motility of differentiated neurons. Cerebral Cortex (New York N.Y.: 1991) 24, 2130–2140.
Costa, A.M., Lucchi, C., Simonini, C., Rosal Lustosa, Í., Biagini, G., 2020. Status epilepticus dynamics predicts latency to spontaneous seizures in the kainic acid model. Cell Physiol. Biochem. 54, 493–507.
Curia, G., Lucchi, C., Vinet, J., Gualtieri, F., Marinelli, C., Torsello, A., Costantino, L., Biagini, G., 2014. Pathophysiogenesis of mesial temporal lobe epilepsy: is prevention of damage antiepileptogenic? Curr. Med. Chem. 21, 663–688.
Devinsky, O., Vezzani, A., O'Brien, T.J., Jette, N., Scheffer, I.E., de Curtis, M., Perucca, P., 2018. Epilepsy. Nat. Rev. Dis. Primers 4, 18024.
Easter, A., Bell, M.E., Damewood, J.R., Redfern, W.S., Valentin, J.-P., Winter, M.J., Fonck, C., Bialecki, R.A., 2009. Approaches to seizure risk assessment in preclinical drug discovery. Drug Discov. Today 14 (17-18), 876–884.
Fezza, F., Marrone, M.C., Avvisati, R., Di Tommaso, M., Lanuti, M., Rapino, C., Mercuri, N.B., Maccarrone, M., Marinelli, S., 2014. Distinct modulation of the endocannabinoid system upon kainic acid-induced in vivo seizures and in vitro epileptiform bursting. Mol. Cell. Neurosci. 62, 1–9.
Fischer, M., Goldschmitt, J., Peschel, C., Brakenhoff, J.P.G., Kallen, K.-J., Wollmer, A., Grötzinger, J., Rose-John, S., 1997. A bioactive designer cytokine for human hematopoietic progenitor cell expansion. Nat. Biotechnol. 15 (2), 142–145.
Gelfman, S., Wang, Q., Lu, Y., Hall, D., Bostick, C.D., Dhindsa, R., Halvorsen, M., McSweeney, K.M., Cotterill, E., Edinburgh, T., Beaumont, M.A., Frankel, W.N., Petrovski, S., Allen, A.S., Boland, M.J., Goldstein, D.B., Eglen, S.J., 2018. meaRtools: an R package for the analysis of neuronal networks recorded on microelectrode arrays. PLoS Comput. Biol. 14, e1006506.
Grainger, A.I., King, M.C., Nagel, D.A., Parri, H.R., Coleman, M.D., Hill, E.J., 2018. In vitro models for seizure-liability testing using induced pluripotent stem cells. Front. Neurosci. 12, 590.
Gruol, D.L., 2015. IL-6 regulation of synaptic function in the CNS. Neuropharmacology 96, 42–54.
Hagman, S., Mäkinen, A., Ylä-Outinen, L., Huhtala, H., Elovaara, I., Narkilahti, S., 2019. Effects of inflammatory cytokines IFN-γ, TNF-α and IL-6 on the viability and functionality of human pluripotent stem cell-derived neural cells. J. Neuroimmunol. 331, 36–45.
Hampel, H., Haslinger, A., Scheloske, M., Padberg, F., Fischer, P., Unger, J., Teipel, S.J., Neumann, M., Rosenberg, C., Oshida, R., Hulette, C., Pongratz, D., Ewers, M., Kretzschmar, H.A., Möller, H., 2005. Pattern of interleukin-6 receptor complex immunoreactivity between cortical regions of rapid autopsy normal and Alzheimer's disease brain. Eur. Arch. Psychiatry Clin. Neurosci. 255, 269–278.
Hirose, S., Tanaka, Y., Shibata, M., Kimura, Y., Ishikawa, M., Higurashi, N., Yamamoto, T., Ichise, E., Chiyonobu, T., Ishii, A., 2020. Application of induced pluripotent stem cells in epilepsy. Mol. Cell. Neurosci. 108, 103535.
Hongisto, H., Ilmarinen, T., Vattulainen, M., Mikhailova, A., Skottman, H., 2017. Xeno- and feeder-free differentiation of human pluripotent stem cells to two distinct ocular epithelial cell types using simple modifications of one method. Stem Cell Res. Ther. 8, 291.

Hyvärinen, T., Hyysalo, A., Kapucu, F.E., Aarnos, L., Vinogradov, A., Eglen, S.J., Ylä-Outinen, L., Narkilahti, S., 2019. Functional characterization of human pluripotent stem cell-derived cortical networks differentiated on laminin-521 substrate: comparison to rat cortical cultures. Sci. Rep. 9, 1–15.

Hyysalo, A., Ristola, M., Mäkinen, M.-L., Häyrynen, S., Nykter, M., Narkilahti, S., 2017. Laminin α5 substrates promote survival, network formation and functional development of human pluripotent stem cell-derived neurons in vitro. Stem Cell Res. 24, 118–127.

Ishibashi, Y., Odawara, A., Kinoshita, K., Okamura, A., Shirakawa, T., Suzuki, I., Affiliations, Suzuki, I., 2021. Principal component analysis to distinguish seizure liability of drugs in human iPS Cell-derived neurons, toxicological studies. Oxford Acad.

Islam, O., Gong, X., Rose-John, S., Heese, K., 2009. Interleukin-6 and neural stem cells: more than gliogenesis. Mol. Biol. Cell 20, 188–199.

Jiruska, P., de Curtis, M., Jefferys, J.G.R., Schevon, C.A., Schiff, S.J., Schindler, K., 2013. Synchronization and desynchronization in epilepsy: controversies and hypotheses. J. Physiol. 591, 787–797.

Kalueff, A.V., Lehtimaki, K.A., Ylinen, A., Honkaniemi, J., Peltola, J., 2004. Intranasal administration of human IL-6 increases the severity of chemically induced seizures in rats. Neurosci. Lett. 365 (2), 106–110.

Kaur, S., Bansal, Y., Kumar, R., Bansal, G., 2020. A panoramic review of IL-6: structure, pathophysiological roles and inhibitors. Bioorg. Med. Chem. 28 (5), 115327.

Kiamehr, M., Klettner, A., Richert, E., Koskela, A., Koistinen, A., Skottman, H., Kaarniranta, K., Aalto-Setälä, K., Juuti-Uusitalo, K., 2019. Compromised barrier function in human induced pluripotent stem-cell-derived retinal pigment epithelial cells from type 2 diabetic patients. Int. J. Mol. Sci. 20, 3773.

Kumar, D., Anand, T., Kues, W.A., 2017. Clinical potential of human-induced pluripotent stem cells: perspectives of induced pluripotent stem cells. Cell Biol. Toxicol. 33, 99–112.

Lappalainen, R.S., Salomäki, M., Ylä-Outinen, L., Heikkilä, T.J., Hyttinen, J.AK., Pihlajamäki, H., Suuronen, R., Skottman, H., Narkilahti, S., 2010. Similarly derived and cultured hESC lines show variation in their developmental potential towards neuronal cells in long-term culture. Regen. Med. 5 (5), 749–762.

Lehtimäki, K.A., Peltola, J., Koskikallio, E., Keränen, T., Honkaniemi, J., 2003. Expression of cytokines and cytokine receptors in the rat brain after kainic acid-induced seizures. Mol. Brain Res. 110 (2), 253–260.

Lehtimäki, K.A., Keränen, T., Palmio, J., Rainesalo, S., Saransaari, P., Peltola, J., 2009. Regulation of cerebrospinal fluid levels of cytokines after seizures: the role of IL-6 and glutamic acid. Eur. J. Neurol. 16.

Lehtimäki, K.A., Liimatainen, S., Peltola, J., Arvio, M., 2011. The serum level of interleukin-6 in patients with intellectual disability and refractory epilepsy. Epilepsy Res. 95 (1-2), 184–187.

Li, G., Bauer, S., Nowak, M., Norwood, B., Tackenberg, B., Rosenow, F., Knake, S., Oertel, W.H., Hamer, H.M., 2010. Cytokines and epilepsy, Seizure: European. J. Epilepsy 20, 249–256.

Lieb, F., Stark, H., Thielemann, C., 2017. A stationary wavelet transform and a time-frequency based spike detection algorithm for extracellular recorded data. J. Neural Eng. 14, 036013.

Liimatainen, S., Fallah, M., Kharazmi, E., Peltola, M., Peltola, J., 2009. Interleukin-6 levels are increased in temporal lobe epilepsy but not in extra-temporal lobe epilepsy. J. Neurol. 256 (5), 796–802.

Liu, Y., Beyer, A., Aebersold, R., 2016. On the dependency of cellular protein levels on mRNA abundance. Cell 165 (3), 535–550.

Liu, J., Sternberg, A.R., Ghiasvand, S., Berdichevsky, Y., 2019. Epilepsy-on-a-chip system for antiepileptic drug discovery. IEEE Trans. Biomed. Eng. 66 (5), 1231–1241.

Lu, J., Zhou, N., Yang, P., Deng, L., Liu, G., 2019. MicroRNA-27a-3p downregulation inhibits inflammatory response and hippocampal neuronal cell apoptosis by upregulating mitogen-activated protein kinase 4 (MAP2K4) expression in epilepsy: in vivo and in vitro studies. Med. Sci. Monit. 25, 8499–8508.

Ma, S.-H., Zhuang, Q.-X., Shen, W.-X., Peng, Y.-P., Qiu, Y.-H., 2015. Interleukin-6 reduces NMDAR-mediated cytosolic Ca2+ overload and neuronal death via JAK/CaN signaling. Cell Calcium 58 (3), 286–295.

Magalhães, D.M., Pereira, N., Rombo, D.M., Beltrão-Cavacas, C., Sebastião, A.M., Valente, C.A., 2018. Ex vivo model of epilepsy in organotypic slices-a new tool for drug screening. J. Neuroinflam. 15, 203.

Mäkinen, M.E., Ylä-Outinen, L., Narkilahti, S., 2018. GABA and gap junctions in the development of synchronized activity in human pluripotent stem cell-derived neural networks. Front. Cell. Neurosci. 12, 56.

Mayer, M., Arrizabalaga, O., Lieb, F., Ciba, M., Ritter, S., Thielemann, C., 2018. Electrophysiological investigation of human embryonic stem cell derived neurospheres using a novel spike detection algorithm. Biosens. Bioelectron. 100, 462–468.

Narkilahti, S., Pirttila, T.J., Lukasiuk, K., Tuunanen, J., Pitkanen, A., 2003. Expression and activation of caspase 3 following status epilepticus in the rat. Eur. J. Neurosci. 18 (6), 1486–1496.

Niu, W., Parent, J.M., 2020. Modeling genetic epilepsies in a dish. Dev. Dyn. 249 (1), 56–75.

Odawara, A., Katoh, H., Matsuda, N., Suzuki, I., 2016. Physiological maturation and drug responses of human induced pluripotent stem cell-derived cortical neuronal networks in long-term culture. Sci. Rep. 6, 26181.

Paavilainen, T., Pelkonen, A., Mäkinen, M.-L., Peltola, M., Huhtala, H., Fayuk, D., Narkilahti, S., 2018. Effect of prolonged differentiation on functional maturation of human pluripotent stem cell-derived neuronal cultures. Stem Cell Res. 27, 151–161.

Pasquale, V., Pasquale, V., Martinoia, S., Martinoia, S., Chiappalone, M., Chiappalone, M., 2010. A self-adapting approach for the detection of bursts and network bursts in neuronal cultures. J. Comput. Neurosci. 29, 213–229.

Patel, D.C., Tewari, B.P., Chaunsali, L., Sontheimer, H., 2019. Neuron-glia interactions in the pathophysiology of epilepsy. Nat. Rev. Neurosci. 20 (5), 282–297.

Pelkonen, A., Mzezewa, R., Sukki, L., Ryynänen, T., Kreutzer, J., Hyvärinen, T., Vinogradov, A., Aarnos, L., Lekkala, J., Kallio, P., Narkilahti, S., 2020. A modular brain-on-a-chip for modelling epileptic seizures with functionally connected human neuronal networks. Biosens. Bioelectron. 168, 112553. https://doi.org/10.1016/j.bios.2020.112553.

Penkowa, M., Molinero, A., Carrasco, J., Hidalgo, J., 2001. Interleukin-6 deficiency reduces the brain inflammatory response and increases oxidative stress and neurodegeneration after kainic acid-induced seizures. Neuroscience 102 (4), 805–818.

Perucca, E., French, J., Bialer, M., 2007. Development of new antiepileptic drugs: challenges, incentives, and recent advances. Lancet Neurol. 6, 793–804.

Rana, A., Musto, A.E., 2018. The role of inflammation in the development of epilepsy. J. Neuroinflam. 15, 144.

Rockley, K.L., Roberts, R.A., Morton, M.J., 2019. Innovative models for in vitro detection of seizure. Toxicol. Res. (Camb.) 8, 784–788.

Rose-John, S., 2017. The soluble interleukin 6 receptor: advanced therapeutic options in inflammation. Clin. Pharmacol. Ther. 102, 591–598.

Rothaug, M., Becker-Pauly, C., Rose-John, S., 2016. The role of interleukin-6 signaling in nervous tissue. BBA 1863 (6), 1218–1227.

Saavedra, L., Wallace, K., Freudenrich, T.F., Mall, M., Mundy, W.R., Davila, J., Shafer, T. J., Wernig, M., Haag, D., 2021. Comparison of acute effects of neurotoxic compounds on network activity in human and rodent neural cultures. Toxicol. Sci. 180, 295–312.

Samland, H., Huitron-Resendiz, S., Masliah, E., Criado, J., Henriksen, S.J., Campbell, I.L., 2003. Profound increase in sensitivity to glutamatergic- but not cholinergic agonist-induced seizures in transgenic mice with astrocyte production of IL-6. J. Neurosci. Res. 73 (2), 176–187.

Schöbitz, B., de Kloet, E.R., Sutanto, W., Holsboer, F., 1993. Cellular localization of interleukin 6 mRNA and interleukin 6 receptor mRNA in rat brain. Eur. J. Neurosci. 5, 1426–1435.

Sirven, J.I., 2015. Epilepsy: a spectrum disorder. Cold Spring Harbor Perspect. Med. 5 (9), a022848.

Skottman, H., 2010. Derivation and characterization of three new human embryonic stem cell lines in Finland. In Vitro Cell. Dev. Biol. -Animal. 46 (3-4), 206–209.

Sulistio, Y., Sulistio, Y., Lee, H., Lee, H., Jung, S., Jung, S., Heese, K., Heese, K., 2018. Interleukin-6-Mediated Induced Pluripotent Stem Cell (iPSC)-Derived Neural Differentiation. Mol. Neurobiol. 55, 3513–3522.

Tukker, A.M., Westerink, R.H.S., 2021. Novel test strategies for in vitro seizure liability assessment. Expert Opin. Drug Metab. Toxicol. 17 (8), 923–936.

Valente, C.A., Meda, F.J., Carvalho, M., Sebastião, A.M., 2021. A model of epileptogenesis in Rhinal cortex-hippocampus organotypic slice cultures. J. Vis. Exp. (169) https://doi.org/10.3791/61330.

Vezzani, A., Balosso, S., Ravizza, T., 2019. Neuroinflammatory pathways as treatment targets and biomarkers in epilepsy, Nature reviews. Neurology. 15 (8), 459–472.

Wolf, J., Rose-John, S., Garbers, C., 2014. Interleukin-6 and its receptors: a highly regulated and dynamic system. Cytokine 70, 11–20.

Zhang, L.I., Poo, M.-ming., 2001. Electrical activity and development of neural circuits. Nat. Neurosci. 4 (S11), 1207–1214.

Zuiki, M., Chiyonobu, T., Yoshida, M., Maeda, H., Yamashita, S., Kidowaki, S., Hasegawa, T., Gotoh, H., Nomura, T., Ono, K., Hosoi, H., Morimoto, M., 2017. Luteolin attenuates interleukin-6-mediated astrogliosis in human iPSC-derived neural aggregates: a candidate preventive substance for maternal immune activation-induced abnormalities. Neurosci. Lett. 653, 296–301.